Physica D 384–385 (2018) 1–11

Contents lists available at ScienceDirect

Physica D

journal homepage: www.elsevier.com/locate/physd

Reconstruction of ensembles of generalized Van der Pol oscillators from vector time series

Ilya V. Sysoev *

Saratov State University, Astrakhanskaya Street, 83, Saratov 410012, Russia
Saratov Branch of Kotel'nikov Institute of Radio Engineering and Electronics of Russian Academy of Sciences, Zelyonaya Street, 38, Saratov 410019, Russia

HIGHLIGHTS

- Ensembles of Van der Pol, Rayleigh and FitzHugh–Nagumo systems are reconstructed.
- The method allows to reconstruct arbitrary nonlinear potential function.
- Linear and nonlinear couplings by coordinate and by derivative were considered.
- High order dissipation functions of individual nodes were approximated and fitted.
- Ensembles up to 128 element were studied in chaotic and periodic regimes.

ARTICLE INFO

Article history:
Received 5 November 2017
Received in revised form 6 July 2018
Accepted 7 July 2018
Available online 7 August 2018
Communicated by A. Pikovsky

Keywords:
Coupling detection
Van der Pol oscillator
Reconstruction from time series
Dynamical systems
Time series analysis

ABSTRACT

The method for reconstruction of nonlinear potential, dissipation and coupling functions for all elements of ensembles of coupled generalized Van der Pol oscillators (including Rayleigh and Bonhoeffer–Van der Pol oscillators) from multivariate time series is proposed.

It is based on the idea of using the smoothness of reconstructed potential function as a criterion for quality of reconstruction. Therefore, no parametrization for potential is required and an arbitrary potential function unique for each oscillator in the ensemble can be considered. Different approaches to reconstruction of dissipation are studied. Linear and nonlinear coupling between oscillators is considered, including coupling by derivatives. Effects of measurement noise, contaminating the series, are taken into account.

1. Introduction

The problem of system reconstruction (also known as system identification) from time series has been well known for many years, and many general and special algorithms were developed. The reviews can be found in [1–3]. The most known approaches can be classified, using the following criteria:

- an approach targets a single dynamical system or a network;
- an approach considers scalar time series (with possible some variables hidden) or vector series;
- an approach targets dynamical systems with possible measurement noise (most methods), or a stochastic differential equations, where noise plays a fundamental role, like [4] (sometimes Bayesian approach is also used to reconstruction of dynamic systems [5]);
- an approach was developed for some general purpose (e. g., see [6]) or for some particular class of systems like nonautonomous ordinary differential equations (ODEs, [7]), time delayed systems [8], or stochastic phase oscillators [9].

The interest to the problem of equation reconstruction (at first, a problem of identification of a single dynamical system) was rising and dropping a number of times in the past. The first results were achieved in [10]. The hidden variable approach [11] gave some hope to reveal dynamics for models well written from the first principles, if some variables are missing. This case is sometimes referenced as "white box", since everything is known about the system except some parameters and some dynamic variables. Then, the more general, but less robust approach was proposed in [6,12], using polynomial approximation and sequential differentiation and/or time delay vector reconstruction. In contrary to the previous one, this case is referenced as "black box" — nothing

* Correspondence to: Saratov State University, Astrakhanskaya Street, 83, Saratov 410012, Russia.
E-mail address: ivssci@gmail.com.

https://doi.org/10.1016/j.physd.2018.07.004
0167-2789/

is actually known except time series. However, both techniques occurred to be hardly to apply to experimental data. This was recognized, and specific techniques for some narrow classes of systems in special cases were developed [13], including nonautonomous systems [7,14] and time delayed systems [8]. Since the approaches based on general functional series for approximation of nonlinear functions are usually very inefficient, some efforts were made for removal of superfluous terms [15]. The number of approaches was developed based on perturbed dynamics, including driving response approaches [16,17] and methods based on transient processes [18].

Recently, a new approach to the problem was proposed in [19–21] for systems, where all dynamical variables are considered to be known, but many different nonlinearities are included in form of a sparse functional matrix. Such an approach can be considered as a new generation of "black box" problem methods, but simpler, since the task of phase vector reconstruction is not considered, and only one derivative is estimated numerically or even measured explicitly. The method [20] allows to reconstruct a network, not only the autonomous system, but the network is actually considered as a single high dimensional oscillator. Also, authors mention that the approach is not efficient for large dimensions due to very fast rise of the problem complexity with an increase of the dimension.

There are also special methods for reconstruction of systems with varying parameters. The early works used the same methods as for stationary systems, but in moving time window [22]. Then, artificial neural networks in combination with the Monte Carlo Markov chain analysis were proposed [23], and a method based on sparse functional matrix fitting [24]. These techniques often aim to predict bifurcation or some other critical behavior.

The fine but not complete reviews of network reconstruction oriented approaches can be found in [25,26]. These techniques can be very relevant for biological applications, especially in neuroscience, where the problem of coupling analysis between different brain regions or between individual neurons is of great importance. Possible applications may also be found in other fields, like radioengineering, climate study, econometrics or social sciences.

Often, network oriented approaches focus mostly on the network structure and consider the equations for individual nodes as simple as possible. In particular, auto-regressive models of first order [27] or Kuramoto-like oscillators [9] are considered. Well known approaches to coupling detection: Granger causality [28] and partial directed coherence [29] are also based on autoregressive models, but some generalizations for nonlinear cases were proposed in [30–32]. Additionally, approaches for nonstationary data were developed in [33,34]. As an exception, a fine technique for reconstruction of a network with Rössler or Lorenz oscillators was proposed in [35], which can be easily generalized for other systems. Use of simple models for nodes limits applicability of these approaches, since the majority of biological or climate studies considers individual subsystems to be complex and multidimensional. Therefore, many researches prefer not to reveal actual physical and structural links and to focus on functional couplings, using the measures of theory of information, like transfer entropy [36], which do not deal with equations for individual nodes at all.

In this study the new, simple and numerically effective approach for reconstruction of networks of generalized Van der Pol oscillators [37] with unknown nonlinear functions is proposed. It is mostly based on the idea of nonparametric reconstruction of a nonlinear function for individual nodes, proposed for two coupled time-delay systems in [8], and generalized for larger ensembles in [38]. This idea aims to reduce the parametrization in comparison to the direct approaches such as [39], for which all nonlinear functions of individual nodes have to be parametrized in order to be reconstructed. Although parametrization is a powerful tool and avoiding it completely is not a good idea in a typical case. In the current work parametrization is used to reconstruct more complex generalizations of Van der Pol oscillator, which include additional nonlinear functions for dissipation and coupling.

Though the proposed technique can be considered as a combination of previously published ideas, it is unique from the point of view of considered object. Van der Pol oscillator is one of the basic models for the theory of oscillations, having many applications. And it is the simplest model in the form of ODEs, being able to demonstrate self-oscillations. The most recent review on this theme can be found in [40]. Generalized Van der Pol oscillator is also popular due to increased number of effects which it can reproduce, see e. g. [41,42]. The examples of biological applications of the generalized Van der Pol oscillator can be seen in the following papers: in [43] generalized Van der Pol oscillator underlies active signal amplification in drosophila hearing; in [44] and [45] generation of electrical activity by neurons and myocytes is modeled by networks of generalized Van der Pol oscillators; a generalized Bonhoeffer–Van der Pol oscillator was reconstructed from data to describe living pacemaker neurons in [46]; in [47,48] Van der Pol oscillators were used for modeling acoustical effects in human vocal folds, in [49] — for modeling absence epileptic seizures.

So, the applicability of generalized Van der Pol equation to the real tasks, possibility to reconstruct the network based on multivariate time series having only one scalar series per each node (the second coordinate can be achieved with numerical differentiation or integration), and number of recent fruitful approaches dealing with networks of first order oscillators like in [50] allow to hope that the current study results will be useful.

2. Method

2.1. Ensemble of coupled oscillators with unknown potential function and original dissipation function

Let us consider an ensemble of diffusely coupled generalized Van der Pol oscillators with arbitrary nonlinear potential functions $f_i(x)$:

$$\ddot{x}_i - \left(r_i - x_i^2\right)\dot{x}_i + f_i(x_i) = \sum_{j=1, j\neq i}^{D} k_{i,j}\left(x_j - x_i\right), \tag{1}$$

where i is a number of an oscillator (node) in the ensemble, r_i is a parameter of linear dissipation ($r_i = 0$ corresponds to Andronov–Hopf bifurcation), and D is a number of nodes.

Let us consider time series $\{x_i(t_n)\}_{n=1}^{N}$ of all D nodes of ensemble to be measured with sampling time Δt, where N is a series length. For simplicity, let us denote $x_i(n) = x_i(t_n)$.

Following [38], let us sort all measured values of $x_i(n)$ and introduce the map $Q_i(n)$, pointing from the number n of a value $x_i(n)$ in the original series to its new number in the sorted one. Actually, it does no matter what algorithm of sorting is used (except maybe calculation time issue). It is also no matters whether sorting is performed by an increase like here, or by a decay. The goal of sorting is to find the data vector which has the x_i value closest to the current one, but simultaneously to guarantee using such a point only once. Otherwise, the additional efforts to avoid linearly interdependent lines in the matrix during least-squares algorithm have to be performed further like in [50]. The sorting is done again for reconstruction of every node, so the measured vectors, corresponding to the considered time moment, are kept unchanged, but sorted by an increase of x_i value, when the reconstruction of ith oscillator is performed. The reverse map would be Q_i^{-1}, leading to $Q_i^{-1}\left(Q_i(n)\right) = n$.

Then, let us consider two sequential values in the sorted series with numbers $Q_i(n)$ and $Q_i(n) - 1$, which have the numbers n and

$p_n = Q_i\big(Q_i(n) - 1\big)$ in the original series. The distance between these values is generally as lesser as larger the length of the series, being very close for sufficient value of N under the obvious assumption that the total series variance is limited.

Let us assume also that the functions f_i are continuous, or they have a finite and small in comparison to N number of discontinuities of the 1st kind. If so, the close values of functions f_i would correspond to the close values of x_i, so, values $f_i\big(x_i(n)\big)$ and $f_i\big(x_i(p_n)\big)$ occur to be very close. Let us denote the difference between them as $\delta_i(n)$:

$$\delta_i(n) = f_i\big(x_i(n)\big) - f_i\big(x_i(p_n)\big). \tag{2}$$

Let us subtract f_i from (1), and then put it to (2), given the following set of equations:

$$f_i(x_i) = -\ddot{x}_i + \left(r_i - x_i^2\right)\dot{x}_i + \sum_{j=1,j\neq i}^{D} k_{i,j}\left(x_j - x_i\right) \tag{3}$$

$$\Delta x_i(n) = x_i(n) - x_i(p_n) \tag{4}$$

$$\Delta \dot{x}_i(n) = \dot{x}_i(n) - \dot{x}_i(p_n) \tag{5}$$

$$\Delta \ddot{x}_i(n) = \ddot{x}_i(n) - \ddot{x}_i(p_n) \tag{6}$$

$$\begin{aligned}\delta_i(n) = &-\Delta\ddot{x}_i(n) - \big(\dot{x}_i(n)x_i^2(n) - \dot{x}_i(p_n)x_i^2(p_n)\big) + \\ &r_i\Delta\dot{x}_i(n) + \sum_{j=1,j\neq i}^{D} k_{i,j}\left(\Delta x_j(n) - \Delta x_i(n)\right).\end{aligned} \tag{7}$$

Let us consider the sum of squares of all $\delta_i(n)$ for the given i as a function of coupling and dissipation parameters $\mathbf{k}_i = \big(k_{i,1}, k_{i,2}, \ldots k_{i,D}\big)$ and r_i:

$$S_i^2(r_i, \mathbf{k}_i) = \sum_{n=1}^{N} \delta_i^2(n), \tag{8}$$

where $Q_i(n) \neq 1$ due to the fact that for this point there is no previous one in the sorted series (the corresponding value is a global minimum of x_i in the whole measures series). This sum is analogous to description length target function used in [8]. The mostly similar idea, actually, was used for neural networks reconstruction in [51], but with a different formalism.

All terms of the sum (8) can be classified to belong to one of two types: first two terms for each $\delta_i(n)$ are constants, the next D terms are a linear combination of known values with unknown coefficients before them (r_i and coupling coefficients $k_{i,j}$, taking into account that $i \neq j$). Since the value S_i^2 should be very small, one can reduce the considered problem of reconstruction to the task of the target function (8) minimization. This task can be solved as a usual linear least-squares problem, i. e. a problem of approximation of values (9) with a linear combinations of values $\Delta\dot{x}_i(n)$ and $\big(\Delta x_j(n) - \Delta x_i(n)\big)$, which could be considered as basis functions.

$$\beta_i(n) = \Delta\ddot{x}_i(n) + \big(\dot{x}_i(n)x_i^2(n) - \dot{x}_i(p_n)x_i^2(p_n)\big) \tag{9}$$

One can easily find that $\lim_{N\to\infty}\delta_i(n) = 0$. However, neither basis functions $\Delta\dot{x}_i(n)$ and $\big(\Delta x_j(n) - \Delta x_i(n)\big)$, nor values $\beta_i(n)$ to be approximated tend to zero with $N \to 0$, since proximity of x_i values in the sorted series does not mean automatically any proximity of time derivatives or values of different x_j. The derivatives and coordinates for different nodes could occur proximate only under generalized synchronization condition.

In the paper [38] the time delay was mentioned as a source of success of the proposed approach. Actually, it was not completely correct, since the time delay was useful but not obligatory assumption.

In summary, one can estimate dissipation parameters r_i and coupling coefficients $k_{i,j}$ by minimizing target function S_i^2 separately for every oscillator in the ensemble. Then, functions f_i can be calculated following formula (3) based on estimated values of r_i and $k_{i,j}$.

2.2. Ensemble of oscillators coupled linearly both by coordinates and velocities

Let us consider the first generalization of the model (1) by introducing additional coupling terms $\big(\dot{x}_j - \dot{x}_i\big)$:

$$\ddot{x}_i - \left(r_i - x_i^2\right)\dot{x}_i + f_i(x_i) = \sum_{j=1,j\neq i}^{D} k_{i,j}\left(x_j - x_i\right) + \sum_{j=1,j\neq i}^{D} k'_{i,j}\left(\dot{x}_j - \dot{x}_i\right). \tag{10}$$

The derivatives $\dot{x}_i$ may be considered as velocities in mechanics or as currents in electrodynamics, if x_i is a coordinate or charge respectively; in neuroscience it could also have some other, less clear meaning.

To solve the reconstruction problem in presence of an additional coupling, let us reformulate (7) by introducing an additional term:

$$\begin{aligned}\delta_i(n) = &-\Delta\ddot{x}_i(n) - \big(\dot{x}_i(n)x_i^2(n) - \dot{x}_i(p_n)x_i^2(p_n)\big) \\ &+ r_i\Delta\dot{x}_i(n) + \sum_{j=1,j\neq i}^{D} k_{i,j}\left(\Delta x_j(n) - \Delta x_i(n)\right) \\ &+ \sum_{j=1,j\neq i}^{D} k'_{i,j}\left(\Delta\dot{x}_j(n) - \Delta\dot{x}_i(n)\right)\end{aligned} \tag{11}$$

Then, the reconstruction can be performed by minimizing the target function (8) similarly to the previously considered case.

2.3. Ensemble of oscillators with unknown potential and dissipation functions

Let us consider another generalization of the model (1), where a dissipation function $g_i(x)$ is unknown:

$$\ddot{x}_i + g_i(x_i)\dot{x}_i + f_i(x_i) = \sum_{j=1,j\neq i}^{D} k_{i,j}\left(x_j - x_i\right). \tag{12}$$

The method can be generalized for this case, if some reasonable approximation is used for $g_i(x)$. The simplest possibilities are either some basis, for example polynomial or trigonometrical, or local linear approximation. In some cases radial or cylinder basis functions could be considered, since they partly combine both approaches. An alternative model-free approach for basis expansion was proposed in [52].

If we consider the polynomial decomposition of $g_i(x)$ into the polynomial (13) of order P, then $\delta_i(n)$ can be rewritten as (14).

$$g_i(x) = \sum_{\nu=0}^{P_g} \rho_{i,\nu}x_i^{\nu}, \tag{13}$$

$$\begin{aligned}\delta_i(n) = &-\Delta\ddot{x}_i(n) - \sum_{\nu=0}^{P_g} \rho_{i,\nu}\left(\dot{x}_i(n)x_i^{\nu}(n) - \dot{x}_i(p_n)x_i^{\nu}(p_n)\right) + \\ &\sum_{j=1,j\neq i}^{D} k_{i,j}\left(\Delta x_j(n) - \Delta x_i(n)\right)\end{aligned} \tag{14}$$

In such a case, the least-squares problem is reformulated as follows: $\Delta\ddot{x}_i(n)$ are values to be approximated instead of $\beta_i(n)$, and the total number of basis functions in (8) increases to $(D + P)$.

If one chooses to use a local linear approximation for g_i, the whole interval of measured values of x_i should be split into L bins, denoted further as $[x_i]_l$, where $l = 1, 2, \ldots, L$. The edges of these bins can be found by making the assumption of their equal length or equal number of points from measured series in all bins. This can be done easily, since the sorted series is already given. Then, $g_i(x)$ can be presented as (15), leading to the formula (17) for $\delta_i(n)$.

$$g_i(x) = \sum_{l=1}^{L} g_{i,l}(x), \tag{15}$$

$$g_{i,l}(x) = \begin{cases} \kappa_{i,l}x + \chi_{i,l}, & \text{if } x \in [x_i]_l, \\ 0, & \text{otherwise.} \end{cases} \tag{16}$$

$$\delta_i(n) = -\Delta\ddot{x}_i(n) - \kappa_{i,l}\left(\dot{x}_i(n)x_i(n) - \dot{x}_i(p_n)x_i(p_n)\right) - \chi_{i,l}\Delta\dot{x}_i(n) + \sum_{j=1,j\neq i}^{D} k_{i,j}\left(\Delta x_j(n) - \Delta x_i(n)\right) \tag{17}$$

Polynomials can behave bad (oscillate a lot) at the ends of the considered intervals. In such a case local linear approximation should be preferred. But one needs to use relatively large number of bins to get a smooth enough approximation, so the number of coefficients would be significantly higher in the common case.

2.4. Ensembles of generalized oscillators with high order dissipation

The method can be adapted to some very well known and important generalizations of Van der Pol oscillator: Rayleigh oscillator [53] and Bonhoeffer–Van der Pol oscillator, also known as FitzHugh–Nagumo model [54,55]. The latter is of the particular interest for neuroscience applications.

Let us consider the following generalization of Eq. (10):

$$\ddot{x}_i + g_i(x_i)\dot{x}_i + g_i'(x_i)\dot{x}_i^3 + g_i''(x_i)\dot{x}_i^5 + f_i(x_i) = \sum_{j=1,j\neq i}^{D} k_{i,j}\left(x_j - x_i\right) + \sum_{j=1,j\neq i}^{D} k'_{i,j}\left(\dot{x}_j - \dot{x}_i\right). \tag{18}$$

Generally, it can be extended even over the cubic term for $\dot{x}_i$ without limitations, but each an additional term would increase the number of coefficients, making the procedure of reconstruction less robust. This generalization directly includes the case of coupled Rayleigh oscillators. The coupled FitzHugh–Nagumo oscillators can be rewritten to this form by the linear change of variables.

All functions $g_i(x)$, $g_i'(x)$, and $g_i''(x)$ have to be approximated explicitly. The piecewise linear approximation analogous to (15), (16) is considered further. For such an approximation the formula for $\delta_i(n)$ can be written as follows:

$$\begin{aligned}\delta_i(n) = {} & -\Delta\ddot{x}_i(n) - \kappa_{i,l}\left(\dot{x}_i(n)x_i(n) - \dot{x}_i(p_n)x_i(p_n)\right) - \chi_{i,l}\Delta\dot{x}_i(n) \\ & - \kappa'_{i,l}\left(\dot{x}_i^3(n)x_i(n) - \dot{x}_i^3(p_n)x_i(p_n)\right) - \chi'_{i,l}\left(\dot{x}_i^3(n) - \dot{x}_i^3(p_n)\right) \\ & - \kappa''_{i,l}\left(\dot{x}_i^5(n)x_i(n) - \dot{x}_i^5(p_n)x_i(p_n)\right) - \chi''_{i,l}\left(\dot{x}_i^5(n) - \dot{x}_i^5(p_n)\right) \\ & + \sum_{j=1,j\neq i}^{D} k_{i,j}\left(\Delta x_j(n) - \Delta x_i(n)\right) \\ & + \sum_{j=1,j\neq i}^{D} k'_{i,j}\left(\Delta\dot{x}_j(n) - \Delta\dot{x}_i(n)\right).\end{aligned} \tag{19}$$

The resulting approach demands to estimate $D \cdot (6 \cdot L + 2 \cdot (D-1))$ coefficients.

2.5. Ensemble with unknown coupling functions

Let us consider that coupling is not linear, but there is some unknown nonlinear function $h(x_j - x_i)$. In contrary to [50], let us consider possibility of different coupling functions for each coupled pair of nodes in each direction. So, Eq. (1) can be rewritten as (20):

$$\ddot{x}_i - (r_i - x_i^2)\dot{x}_i + f_i(x_i) = \sum_{j=1,j\neq i}^{D} h_{i,j}\left(x_j - x_i\right), \tag{20}$$

Each coupling function $h_{i,j}$ can be decomposed. Local linear approximation is not suitable for coupling functions, since all $(D-1)$ differences $(x_j - x_i)$ must be sorted and separate bins must be established. This will cause very large segmentation. Actually, this is similar to establishing bins in $(D-1)$-dimensional space. Therefore, let us limit our consideration to the polynomial decomposition of form (21) only.

$$h_{i,j}(x) = \sum_{\nu=1}^{P_h} \gamma_{i,j,\nu}x^{\nu} \tag{21}$$

Constant term in the decomposition (21) can be neglected, since it must be the same for all $h_{i,j}$ with the same i (otherwise we will face a problem of linear interdependence). Moreover, the proposed technique is not able to determine a constant shift in coupling function, since constant terms for all $x_i(n)$ and $x_i(p_n)$ are the same. Therefore, these terms are canceled in the formula for $\delta_i(n)$.

Considering the original dissipation function (20) and polynomial approximation for g_i, formula for $\delta_i(n)$ can be rewritten as follows:

$$\delta_i(n) = -\Delta\ddot{x}_i(n) + \left(\dot{x}_i(n)x_i^2(n) - \dot{x}_i(p_n)x_i^2(p_n)\right) + r_i\Delta\dot{x}_i(n) + \sum_{j=1,j\neq i}^{D}\sum_{\nu=1}^{P_h}\gamma_{i,j,\nu}\left(\left(x_j(n) - x_i(n)\right)^{\nu} - \left(x_j(p_n) - x_i(p_n)\right)^{\nu}\right). \tag{22}$$

Let us also consider the more general case, when neither potential function $f_i(x)$, nor dissipation function $g_i(x)$, nor coupling functions $h_{i,j}(x)$ are known. In this case the ensemble equations can be written as (23):

$$\ddot{x}_i + g_i(x)\dot{x}_i + f_i(x_i) = \sum_{j=1,j\neq i}^{D} h_{i,j}\left(x_j - x_i\right). \tag{23}$$

Using polynomial decomposition of dissipation function (14) and polynomial decomposition of coupling functions (21), the differences $\delta_i(n)$ are reformulated as follows:

$$\delta_i(n) = -\Delta\ddot{x}_i(n) + \sum_{\nu=0}^{P_g}\rho_{i,\nu}\left(\dot{x}_i(n)x_i^{\nu}(n) - \dot{x}_i(p_n)x_i^{\nu}(p_n)\right) + \sum_{j=1,j\neq i}^{D}\sum_{\nu=1}^{P_h}\gamma_{i,j,\nu}\left(\left(x_j(n) - x_i(n)\right)^{\nu} - \left(x_j(p_n) - x_i(p_n)\right)^{\nu}\right). \tag{24}$$

So, the problem is reduced to a least-squares problem with $\left(P_h(D-1) + P_g + 1\right)$ unknown coefficients.

Using the local linear approximation for the dissipation function (15), the differences $\delta_i(n)$ are rewritten as follows:

$$\delta_i(n) = -\Delta\ddot{x}_i(n) + \kappa_{i,l}\left(\dot{x}_i(n)x_i(n) - \dot{x}_i(p_n)x_i(p_n)\right) + \chi_{i,l}\Delta\dot{x}_i(n) + \sum_{j=1,j\neq i}^{D}\sum_{\nu=1}^{P_h}\gamma_{i,j,\nu}\left(\left(x_j(n) - x_i(n)\right)^{\nu} - \left(x_j(p_n) - x_i(p_n)\right)^{\nu}\right), \tag{25}$$

where l is determined by the (16). So, the problem is reduced to least-squares with $(P_h(D-1) + 2L)$ unknown coefficients.

3. Results

To test the proposed approach, the numerical simulations of ensembles of all considered in the previous section generalizations

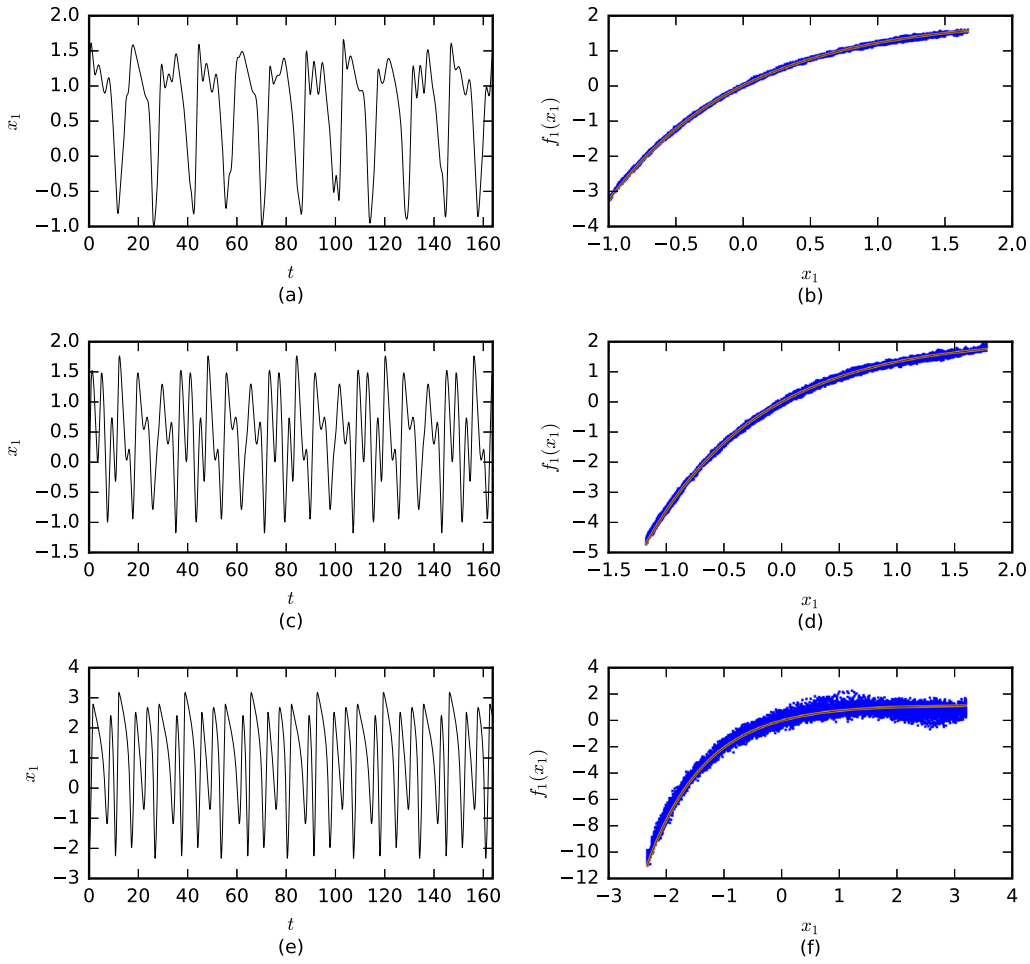

Fig. 1. Panels (a, c, e): time series of oscillator No 1 from the ensemble of $D = 16$ oscillators. Panels (b, d, f): the nonlinear potential function f_1, black line depicts the original function, orange line depicts the function reconstructed in absence of measurement noise (it was specially plotted thicker), and blue dots correspond to the function reconstructed from series contaminated with the measurement noise with standard deviation equal to 0.002. Panels (a, c) correspond to the original ensemble (1) in a chaotic regime, panels (b, d) — to the ensemble (10) with the additional coupling by derivatives also in a chaotic regime, panels (e, f) correspond to a periodic regime in the original ensemble (1). (For interpretation of the references to color in this figure legend, the reader is referred to the web version of this article.)

of Van der Pol oscillator were performed for different number of nodes.

3.1. Reconstruction of ensemble with the original dissipation function and linear coupling

For the original oscillator (1) coupling matrices were generated for different number of nodes D, varying from 4 to 64. Only ensembles demonstrating chaotic behavior were considered for reconstruction. The potential functions f_i were set to the Toda function (26).

$$f_i(x) = \omega_i^2\left(1 - e^{-x}\right), \tag{26}$$

where ω_i are frequencies of small, quasiharmonic oscillations chosen randomly from the uniform distribution in the interval [0.4; 1.46], and parameters r_i were chosen from uniform distribution in the interval [0.1; 1.1]. Such a potential cannot be approximated by a polynomial of finite order precisely, so the proposed technique with nonparametrical estimation makes an additional sense. Interestingly, Van der Pol oscillator with such a potential was considered as a model of a laser in [56].

Coupling coefficients $k_{i,j}$ were generated from uniform distribution with zero low bound and standard deviation equal to $J/\sqrt{D}$, where $J = 0.5$ in most considered cases.

Equations were solved using standard 4th order Runge–Kutta algorithm with sampling time interval $\Delta t = 0.01$. The transient process of length of $N_{trans} = 2^{15}$ sampling time intervals was missed. Vector time series of length $N = 2^{14}$ from all ensemble elements were recorded. Time series of one node of an ensemble composed from $D = 16$ oscillators are shown in Fig. 1(a).

The reconstruction procedure described in the Section 2.1 was applied. Since the method should be sensitive to the noise, series contaminated with a measurement noise (noise realizations were simply added to the already generated series) were considered. To estimate the derivatives in such a case, the Savitzky–Golay filter [57] of the second order was used with different number of points m in a smoothing window. The low temporal resolution is well known source of spurious causality [58]. In the considered examples there was at least 60 data point per one oscillation.

To estimate the quality of reconstruction of individual nodes, reconstructed nonlinear functions were compared to the original ones (see 1(b) in both cases: without noise and for noise contaminated series. One can see a good correspondence of the original functions to the reconstructed ones.

To estimate the quality of reconstruction of coupling coefficients, the distribution of relative errors of coupling estimates $\Delta\tilde{k}_{i,j} = 1 - \tilde{k}_{i,j}/k_{i,j}$ was calculated, where $\tilde{k}_{i,j}$ are obtained with the proposed method and $k_{i,j}$ are the original values. The distribution was plotted for the whole ensemble (240 coefficients in total) in

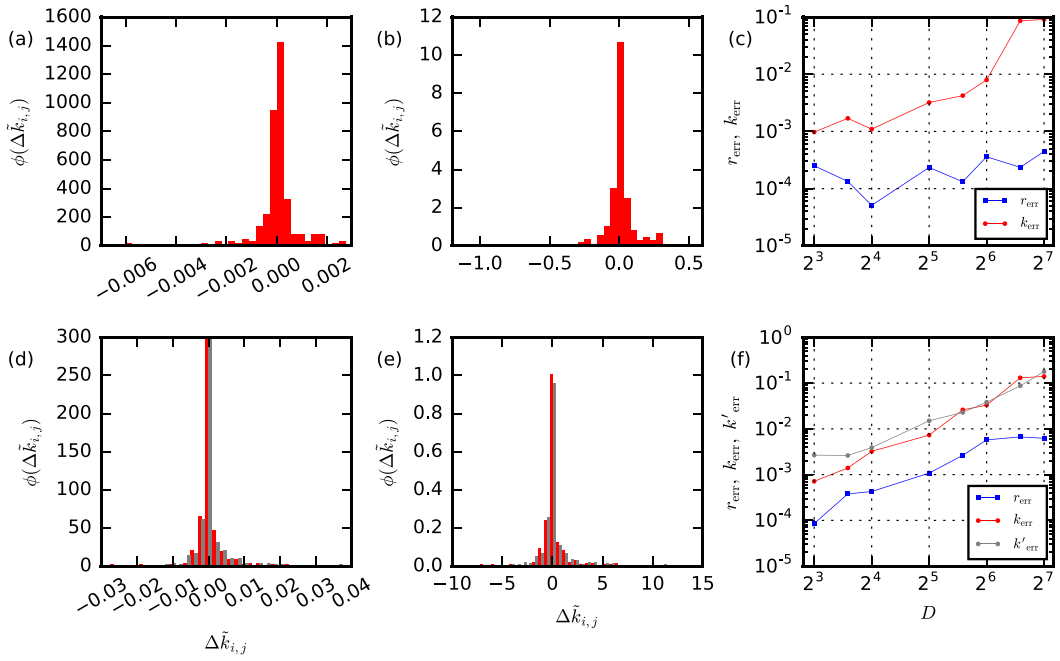

Fig. 2. Panels (a, d): the distribution density of relative errors of estimates of coupling coefficients for an ensemble of $D = 16$ oscillators. The panel (a) corresponds to the original oscillator (1), while panel (d) corresponds to the oscillator with additional coupling by derivative (10), for which errors in $k_{i,j}$ are indicated in red and errors in $k'_{i,j}$ are indicated in gray. Panels (b, e): the same distribution density in case of series contaminated by a measurement noise with the standard deviation 0.002. Panels (c, f): dependence of a mean relative errors in estimation of coupling coefficients $\tilde{k}_{i,j}$ and dissipation parameters $\tilde{r}_i$ on the number D of oscillators in the ensemble. Panels (a, b, c) correspond to the case of coupling only by coordinate, see Eq. (1); panels (d, e, f) correspond to the double coupling by coordinate and first derivative, see Eq. (10). (For interpretation of the references to color in this figure legend, the reader is referred to the web version of this article.)

Fig. 2(a) and 2(b) for clear and noise contaminated series respectively. The value ± 1 corresponds to 100% error in coupling coefficient estimation. One can see that for clear series the errors are very small. For contaminated series they are significantly higher, but nevertheless, more than 90% of coefficients were reconstructed with errors less than 10%.

To understand how the errors of estimation of coupling coefficients and dissipation parameters behave for different number of nodes, the reconstruction was performed for $D = 8,\ 12,\ 16,\ 32,\ 48$ and 64 nodes. Four different ensembles with different coupling matrices and different original parameters r_i and ω_i were considered for each D. The mean relative errors for r_i and $k_{i,j}$ were calculated following formulas (27) and (28) respectively.

$$r_{\rm err} = \left\langle \left| \frac{r_i - \tilde{r}_i}{r_i} \right| \right\rangle_{i=1,\ldots,D}, \tag{27}$$

$$k_{\rm err} = \left\langle \left| \frac{k_{i,j} - \tilde{k}_{i,j}}{k_{i,j}} \right| \right\rangle_{i,j=1,\ldots,D,\ i\neq j}, \tag{28}$$

where $\tilde{r}_i$ are estimates. Resulting mean errors $r_{\rm err}$ and $k_{\rm err}$ were plotted in Fig. 2(c) for different D. One can see that an error $k_{\rm err}$ is increasing with an increase of number of nodes. This effect should be expected due to the rise of the number of coupling coefficients to be estimated per each scalar series. The particular oscillation regime in the ensemble also plays some role. Generally, the higher is the first Lyapunov exponent in the ensemble, the smaller are errors of reconstructed coupling coefficients and dissipation parameters.

In the presence of contaminating noise, the number of points m (smoothing time window length for Savitzky–Golay filter used for numerical estimation of derivatives) becomes important. For different oscillators in the ensemble the optimal m value can be different; it can be found empirically taking into account that the better estimates usually occur for the lower value of the target function (8).

3.2. Reconstruction of ensembles with two types of coupling

For the case of ensemble with two types of coupling (10), coupling coefficients $k_{i,j}$ were generated from the uniform distribution with the zero mean and the standard deviation equal to $J/\sqrt{D}$, and coupling coefficients $k'_{i,j}$ — from the normal distribution with the zero mean and the same standard deviation $J/\sqrt{D}$, with $J = 0.3$. The typical time series of oscillations can be seen in Fig. 1(c). The measurement noise with standard deviation of 0.002 was added to series of all nodes after the simulation.

The reconstructed nonlinear function was plotted in Fig. 1(d). The errors of nonlinear function reconstruction in presence of noise were larger than for the case of oscillators coupled only via coordinates (1). However, the quality of reconstruction changed from one oscillator to another in the ensemble, and it was different for different ensembles. Four different ensembles were generated for different number of nodes $D = 8,\ 12,\ 16,\ 32,\ 48$ and 64. Different random coupling matrices and different random dissipation parameters r_i were studied.

To characterize the average precision of reconstructed coefficients r_i and $k_{i,j}$, the formulas (27) and (28) were used. The mean relative error for reconstructed values of coefficients $k'_{i,j}$ was established similarly, following Eq. (29).

$$k'_{\rm err} = \left\langle \left| \frac{k'_{i,j} - \tilde{k}'_{i,j}}{k'_{i,j}} \right| \right\rangle_{i,j=1,\ldots,D,\ i\neq j}. \tag{29}$$

These estimates were plotted in Fig. 2(f). The distributions of parameter estimate errors for all elements of an ensemble of 16 oscillators were plotted in Fig. 2(d) in absence of measurement noise and in 2(e) in presence of measurement noise, which was distributed normally with the zero mean and the standard deviation equal to 0.002. Errors for coefficients $k_{i,j}$ were plotted in red, and errors for coefficients $k'_{i,j}$ were plotted in gray. The errors without noise are negligible. But even in the presence of noise, more than

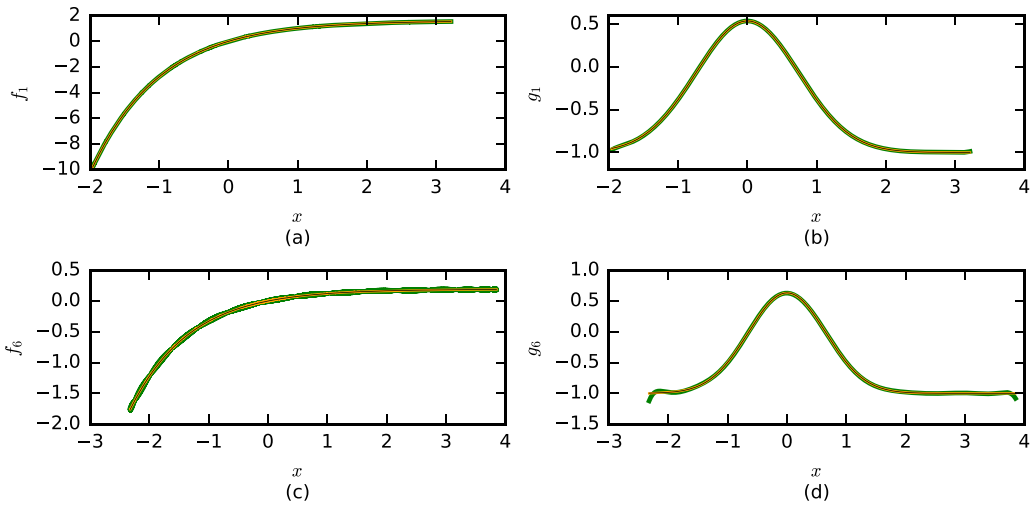

Fig. 3. Panels (a,c): results of reconstruction of potential function f_i, black line shows the original function, orange line (specially plotted thicker) shows the results of reconstruction using local linear approximation of g, green line (specially plotted even more thicker) shows the results reconstructed using the polynomial approximation of g; panels (a) and (c) were plotted for two different oscillators of the ensemble of 8 nodes. Panels (b,d) show the result of reconstruction of dissipation function g for the same oscillators with the same meaning for colors. (For interpretation of the references to color in this figure legend, the reader is referred to the web version of this article.)

80% of coefficients are reconstructed with the relative error equal to 0.25% or less.

Interestingly, there was no significant difference between precision in reconstructed values of $k_{i,j}$ and $k'_{i,j}$ even in the presence of noise, but errors occurred to be much larger for the ensemble (10) than for the ensemble (1). This means that the total number of coefficients to be estimated is more important and the error in estimation of the first derivative is negligible in comparison to the error in estimation of the second one.

The average errors (27)–(29) increased with the number of oscillators in the ensemble D at the constant time series length N (see Fig. 2(f)), what was predictable.

3.3. Reconstruction of ensembles with unknown dissipation function and linear couplings

To illustrate the efficiency of the method in the case of arbitrary unknown dissipation function g_i, the Gaussian (30) was used as g_i, since such a function allows to establish regimes similar to the original ones.

$$g_i(x) = r_i - \mu_i \left(1 - e^{-x^2/\sigma_i^2}\right). \tag{30}$$

The function (30) can be decomposed into an infinite polynomial series.

The same values of the sampling time Δt, the series length N and the transient process length N_{trans} were considered, as above. Values r_i were similarly randomly obtained from the uniform distribution in the interval [0.1; 1.1]. Values of parameters μ_i were chosen as $\mu_i = 1 + r_i$ in order to achieve robust generation. Values of parameters σ_i were obtained randomly from the uniform distribution in the interval [0.8; 1.2].

Fig. 3 shows the results of reconstruction of potential functions f_i and dissipation functions g_i using the polynomial approximation for g_i (green curves) and the local linear approximation (orange curves). The polynomial order $P_g = 12$ was chosen as leading to the minimal values of target function (8). Generally, both functions f and g occur to be reconstructed fine. However, for some nodes in the ensemble the polynomial approximation leads to oscillating tails, as it can be clearly seen from Fig. 3(d). The thickness of the estimated function f_6 oscillate due to these oscillating tails. Note that following the proposed approach, f was not decomposed into a series, but calculated using formula similar to (3) after all parameters had been estimated.

The local linear approximation of g allows to get better results in comparison to the polynomial one in some cases: see e. g. Fig. 3(c, d) for oscillator No 6. But one has to pay for this by an increased number of coefficients in the model. In particular, in the example provided the number of bins $L = 64$, so the total number of coefficients was $D(D-1)+2L = 184$. At the same time, the polynomial approximation demanded only $D(D-1)+P_g+1 = 69$ coefficients. The target function values occur to be very similar for both types of approximation for 5 oscillators from 8 in ensemble, but for three others including oscillator No 6 the resulting target function value for the polynomial approximation was 10–20 times higher.

Actually, the preferable type of approximation for g cannot be guessed a priori. But the value of a target function can be considered as a marker for a better choice. Also, the individual consideration for each oscillator can be preferred. This is not very time consuming and can be performed automatically, since reconstruction is done using ordinary linear least-squares routine which has a number of very efficient realizations. The most time consuming part of the procedure is usually an application of Savitzky–Golay filter, but it can be easily moved to GPU.

3.4. Reconstruction of ensembles of oscillators with the high order dissipation

Reconstruction of the ensemble of oscillators (18) with the high order dissipation coupled both by coordinate and velocity is interesting, complex and very relevant for practical applications, since Rayleigh and FitzHugh–Nagumo systems become included into the consideration. To study it, the functions g_i were chosen to be same as in the previously considered case, see formula (30). The functions $g'_i(i)$ and $g''_i(x)$ were considered as second order polynomials of the form

$$g'_i(x) = \gamma'_i + \alpha'_i x^2, \tag{31}$$

$$g''_i(x) = \gamma''_i + \alpha''_i x^2, \tag{32}$$

where all coefficients γ'_i, γ''_i, α'_i and α''_i were chosen randomly from the uniform distribution with the parameters [0, 0.5]. Such a choice corresponds to the case of "normal", i. e. positive dissipation. Ensembles of $D = 8$ and $D = 16$ oscillators were studied.

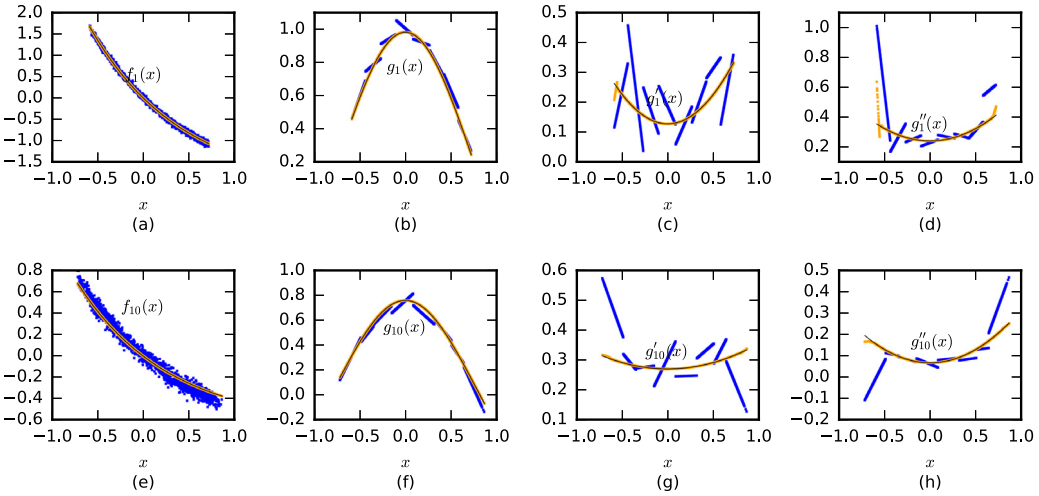

Fig. 4. Results of reconstruction for two oscillators from the ensemble of $D = 16$ oscillators of type (18), i.e. with high order dissipation and coupling both by coordinate and velocity. The upper row (panels a–d) corresponds to the oscillator No 1, the lower row (panels e–h) corresponds to the oscillator No 10. Panels (a, e) show the results of potential function $f_i(x)$ reconstruction, panels (b, f) show the results of dissipation function $g_i(x)$ reconstruction, panels (c, g) and (d, h) show the results of reconstruction of high order dissipation functions $g_i'(x)$ and $g_i''(x)$. The original functions were plotted in black, the functions reconstructed from clear series were plotted in orange thick, the functions reconstructed from noisy series were plotted in blue. (For interpretation of the references to color in this figure legend, the reader is referred to the web version of this article.)

Vector time series of $N = 2^{14}$ points were used similarly to all previous cases. The additive measurement normal noise with the zero mean and the standard deviation 0.002 was added to simulated series.

The results of reconstruction of all functions: potential function $f(x)$, dissipation function $g(x)$, and high order dissipation functions $g'(x)$, $g''(x)$ were plotted in Fig. 4 for absence of noise (orange lines) and in presence of noise (blue lines) for two different oscillators. The local linear approximation was used for dissipation functions. $L = 64$ was used in cases of clear series, but $L = 8$ was used for noisy series to improve the statistical properties of coefficient estimates. One can see that potential function and main dissipation function g were reconstructed mostly acceptable even in the case of noise. The high order dissipation functions were also reconstructed fine without noise, but for the noise present there were significant errors in reconstruction of them, especially at the boundary segments of the x range.

The coupling coefficients for mostly all oscillators are reconstructed fine in absence of noise, the errors are at the similar level as those presented in Fig. 2. When the noise was added, the coefficients were reconstructed with large errors. The relatively good reconstruction of individual potential and dissipation function together with the bad reconstruction of coupling coefficients can be a result of partial synchronization, since many couplings occur to be interchangeable by their effect due to the similar dynamics of the driving nodes. Interestingly, for one oscillator, where most couplings were small except 5, the quality of reconstruction of these 5 relatively large coupling coefficients was high: $\Delta\tilde{k}_i$, $\Delta\tilde{k}'_i \in [0, 0.2]$.

3.5. Reconstruction of ensembles with unknown coupling functions

To demonstrate the method applicability for the case of unknown nonlinear coupling functions $h_{i,j}$, the arc-tangent coupling functions (33) were chosen, since sigmoid functions are usually considered in neuroscience.

$$h_{i,j}(x) = k_{i,j} \arctan(x), \tag{33}$$

where coefficients $k_{i,j}$ were generated similarly to previously considered cases.

For the original dissipation function of Van der Pol oscillator, $\delta_i(n)$ can be written as (22). The results of coupling function approximation were plotted in Fig. 5(a, b) for an ensemble of 8 nodes for two different coupling functions. Polynomial approximation for $h_{i,j}$ with polynomial order $P_h = 11$ was used for all 56 unknown coupling functions. Better approximation of coupling function is achieved for larger coupling coefficients $k_{i,j}$, e. g. compare Fig. 5(a) and (b). This is not surprising, since in this case the impact of the driving into the dynamics of reconstructed nodes is larger. Better reconstruction for weak couplings can be achieved using longer series. Also, polynomial oscillations at both edges of the range can be clearly see in Fig. 5(b).

For the most general case, when neither coupling functions, nor dissipation functions were known, the results of reconstruction of coupling functions were plotted in Fig. 5(c, d) for an ensemble of 8 oscillators. The local linear approximation with $L = 64$ bins was used for dissipation function in the considered case. The quality of results is mainly similar to the case of original dissipation.

3.6. Dependence of results on the time series length

Reconstruction of large ensembles of tens and hundreds of oscillators demands a lot of data, otherwise the problem of coupling coefficient estimation and the problem of reconstruction of self nonlinear functions of individual nodes occurs to be ill defined. In this subsection, the proposed method is tested for different time series length. The networks of original generalized oscillators (1) and oscillators with an additional coupling by derivative (10) were studied. For them the mean errors of estimation of nonlinearity parameter r_i and coupling coefficients $k_{i,j}$ and $k'_{i,j}$ were calculated using formulas (27)–(29) respectively. Results were plotted in Fig. 6.

The coupling coefficients $k_{i,j}$ and $k'_{i,j}$ have larger relative errors than the nonlinearity parameter r_i. This can be explained by the larger role of r_i for the dynamics, since it influences both amplitude and frequency of oscillations, while different couplings can partly interfere due to partial synchronization, and therefore, an error in one coefficient can be partly compensated by an error in another.

Also, the dependences of errors over N for periodic regime (see Fig. 6(c, d)) are usually more flat than for chaotic ones (Fig. 6(c, d)). This is not surprising, since periodic regimes do not provide many

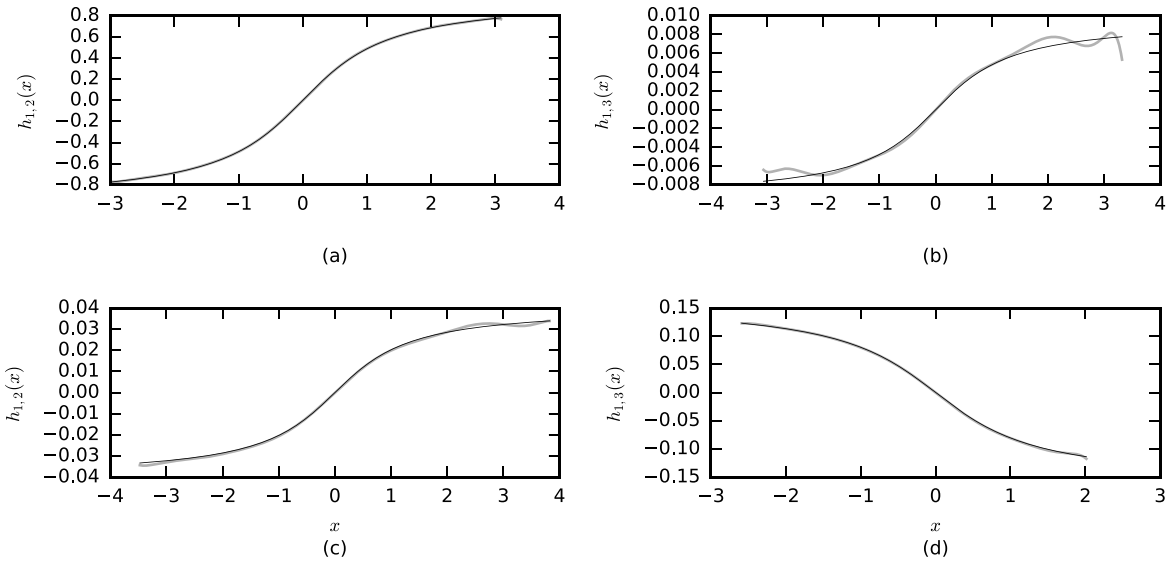

Fig. 5. Results of reconstruction of coupling functions for the ensembles of $D = 8$ oscillators. Original functions were plotted in black, reconstructed functions were plotted in gray thick. Panels (a,b) correspond to the ensemble of type (20) — with the original dissipation function, two different coupling functions. Panels (c,d) correspond the ensemble of type (23) — with unknown dissipation function (actually Gaussian), also two different coupling functions for the same oscillator. Polynomial order $P_h = 11$ was used in all cases.

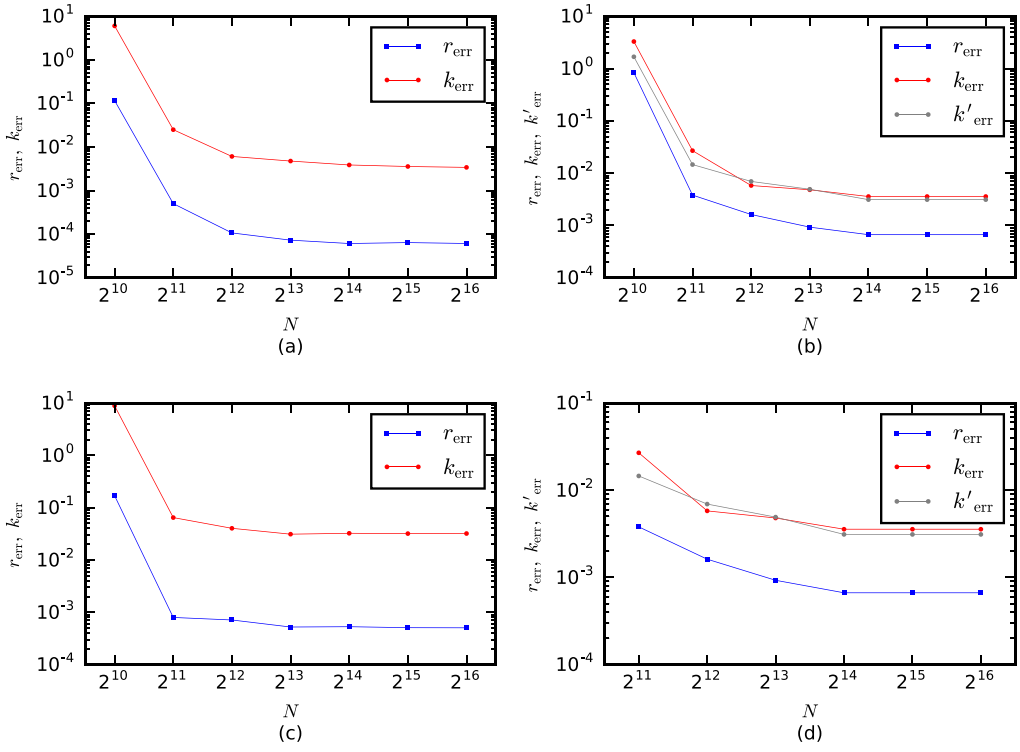

Fig. 6. Dependence of reconstruction mean errors for nonlinearity coefficients r_i and coupling coefficients $k_{i,j}$ and $k'_{i,j}$ on time series length. Subplots (a, c) correspond to the ensemble of original oscillators (1), while subplots (b, d) correspond to the modified network with additional couplings by derivative (10). Subplots (a, b) show results for chaotic series and subplots (c, d) — for periodic ones.

new information for reconstruction after one period is taken into account. The possible improvement can be achieved only due to better averaging and noise reduction, and due to the fact that the sampling interval and the period of oscillations are not in an integer ratio in generally.

Since the number of coupling coefficients rises as $O(D^2)$, while the amount of data is proportional to $(N \cdot D)$, and therefore rises as $O(D)$ with increase of the number of oscillators D, the longer series are usually necessary for larger networks.

4. Discussion and conclusion

The idea of reconstruction of mathematical models from experimental time series and the idea of coupling estimation from time series of activity of two or more systems are very old and overlap a lot. Reconstruction of nonautonomous [7] or coupled [8] oscillators always means that the coupling is estimated in addition to the individual dynamics. And using forecasting models for coupling estimation, as it was proposed by Wiener [59] and Granger [28],

always implies that some individual dynamics for each considered system is modeled.

But actual realizations of these two ideas are mostly different for many years. While the original work of Granger did not limit the type of models used for coupling detection, pretty all known implementations are based on different autoregressive models, which can be considered as stochastic maps in terms of nonlinear dynamics. In contrary, ordinary differential equations [10] are considered in the field of model reconstruction from the beginning, because ODEs are mostly used in many fields of physics, including biophysics, while papers on reconstruction of maps and time-delayed equations are also known. Reconstruction of partial differential equations is usually considered to be too complex, or systems described by them are substituted by networks of smaller subsystems, described by ODEs.

The separation of coupling detection and system identification methods has a significant reason. When reconstructing couplings, dealing with nodes described by relatively complex equations is always disadvantageous, since the individual parameters and nonlinear functions of nodes have to be reconstructed in addition to the coupling. Therefore, these functions are usually considered to be known, like in [35]. But for experimental data these functions are usually unknown. The approximation by polynomials and trigonometric functions is also possible like in [6,7,39]. But decomposition of unknown functions into some basis usually leads to significant (and even dramatic) increase in number of unknown coefficients, and therefore makes results not robust enough.

The other problem is that reconstruction of complex models for individual nodes, composed of multiple equations, demands series of multiple variables to be measured simultaneously for each node. Approaches oriented to reconstruction in the presence of hidden variable behave well when they deal with a single system with well known structure, as in [11], but they occur to be not applicable for an ensemble of such systems with hidden variables per each node.

Thus, existing approaches [29–31,36,33,34,60] made a significant impact into the knowledge of network organization in neuroscience [61–66], climate science [67,68], social sciences [69]. But difficulties of interpretation of their results still demand the intense development in the field.

The possible way to advance is to use approaches which do not demand the explicit parametrization of nonlinear functions of individual nodes or coupling functions, like in [50]. Instead, a technique may focus on smoothness of these functions as a criterion for their correct estimation or some other targets. Such an approach was suggested in the current paper for coupled generalized Van der Pol oscillators. To increase generality, the combined technique, in which potential function is reconstructed implicitly, but the dissipation function (or functions) and the coupling functions are parametrized explicitly, was also considered. In addition, the generalized case, including variously coupled Rayleigh oscillators, and Bonhoeffer–Van der Pol oscillators (also known as FitzHugh–Nagumo equation) was studied. The quality of reconstruction occurred to be acceptable for most considered cases except for some links, corresponding to very small coupling terms.

The limitation of the proposed approach is that it is still sensitive to measurement noise, especially for large ensemble size, because noise reduces the amount of information about an ensemble and because the second derivative has to be estimated. This limitation originates from the idea to use sequential differentiation as a way to reconstruct state vector, which is general for many other previously proposed approaches for ODE reconstruction, see for instance [6,7]. However, if one can measure derivatives explicitly, the problem can be eliminated or at least significantly reduced. The situation when the first or second derivative is the only measured signal is also possible; in such a case numerical integration should be performed for vector state reconstruction, which is not so sensitive to noise as numerical differentiation. Also, for the relatively small ensembles of 8–16 nodes even the proposed approach occurs to be efficient enough for medium noise level.

Acknowledgment

This research was funded by Russian Science Foundation, Grant No. 14-12-00291.

References

[1] G. Gouesbet, G. Meunier-Guttin-Cluzel, O. Menard, Chaos and its Reconstruction, Nova Science Publishers, New York, 2003.
[2] B.P. Bezruchko, D. a. Smirnov, Extracting Knowledge From Time Series: (An Introduction to Nonlinear Empirical Modeling), in: Springer Series in Synergetics, Springer, New York, 2010.
[3] W.X. Wang, Y.C. Lai, C. Grebogi, Data based identification and prediction of nonlinear and complex dynamical systems, Phys. Rep. 644 (2016) 1–76. http://dx.doi.org/10.1016/j.physrep.2016.06.004.
[4] Y.I. Molkov, E.M. Loskutov, D.N. Mukhin, A.M. Feigin, Random dynamical models from time series, Phys. Rev. E 85 (2012) 036216. http://dx.doi.org/10.1103/PhysRevE.85.036216.
[5] D.N. Mukhin, A.M. Feigin, E.M. Loskutov, Y.I. Molkov, Modified Bayesian approach for the reconstruction of dynamical systems from time series, Phys. Rev. E 73 (2006) 036211. http://dx.doi.org/10.1103/PhysRevE.73.036211.
[6] G. Gouesbet, C. Letellier, Global vector-field reconstruction by using a multivariate polynomial l2 approximation on nets, Phys. Rev. E 49 (1994) 4955.
[7] B.P. Besruchko, D.A. Smirnov, Constructing nonautonomous differential equations from experimental time series, Phys. Rev. E 63 (2000) 016207.
[8] M. Prokhorov, V. Ponomarenko, Estimation of coupling between time-delay systems from time series, Phys. Rev. E 72 (2005) 016210.
[9] D.A. Smirnov, B.P. Bezruchko, Detection of coupling in ensembles of stochastic oscillators, Phys. Rev. E 79 (2009) 046204.
[10] J. Cremers, A. Hbler, Construction of differential equations from experimental data, Z. Nat.forsch. 42 (8) (1987) 797–802.
[11] E. Baake, M. Baake, H. Bock, K. Briggs, Fitting ordinary differential equations to chaotic data, Phys. Rev. A 45 (8) (1992) 5524–5529.
[12] V.S. Anishchenko, A. Pavlov, N. Janson, Global reconstruction in the presence of a priori information, Chaos Solitons Fractals 9 (8) (1998) 1267–1278.
[13] B.P. Bezruchko, Y.P. Seleznev, V.I. Ponomarenko, M.D. Prokhorov, D.A. Smirnov, T.V. Dikanev, I.V. Sysoev, A.S. Karavaev, Special approaches to global reconstruction of equations from time series, Izvestiya VUZ. Applied Nonlinear Dynamics (Izvestiya Vysshikh Uchebnykh Zavedeniy. Prikladnaya Nelineynaya Dinamika) 10 (3) (2002) 137–158.
[14] D.A. Smirnov, I.V. Sysoev, E.P. Seleznev, B.P. Bezruchko, Global reconstruction from nonstationary data, Tech. Phys. Lett. 29 (10) (2003) 824827. http://dx.doi.org/10.1134/1.1623857.
[15] A. Severyuknina, Optimization of basis function set for model map reconstruction of short electroencephalogram tracings during epileptic seizure, Izvestiya VUZ. Applied Nonlinear Dynamics (Izvestiya Vysshikh Uchebnykh Zavedeniy. Prikladnaya Nelineynaya Dinamika) 21 (3) (2013) 88–95.
[16] M. Timme, F. Wolf, T. Geisel, Prevalence of unstable attractors in networks of pulse-coupled oscillators, Phys. Rev. Lett. 89 (2002) 154105. http://dx.doi.org/10.1103/PhysRevLett.89.154105.
[17] P. Menck, J. Heitzig, N. Marwan, J. Kurths, How basin stability complements the linear-stability paradigm, Nat. Phys. 9 (2013) 8992. http://dx.doi.org/10.1038/nphys2516.
[18] B.P. Bezruchko, T.V. Dikanev, D.A. Smirnov, Role of transient processes for reconstruction of model equations from time series, Phys. Rev. E 64 (2001) 036210.
[19] X. Han, Z. Shen, W.X. Wang, Z. Di, Robust reconstruction of complex networks from sparse data, Phys. Rev. Lett. 114 (2015) 28701. http://dx.doi.org/10.1103/PhysRevLett.114.028701.
[20] S. Brunton, J. Proctor, J. Kutz, Discovering governing equations from data by sparse identification of nonlinear dynamical systems, Proc. Natl. Acad. Sci. USA 113 (2016) 39327. http://dx.doi.org/10.1073/pnas.1517384113.
[21] N. Mangan, S. Brunton, J. Proctor, J. Kutz, Inferring biological networks by sparse identification of nonlinear dynamics, IEEE Trans. Mol. Biol. Multi-Scale Commun. 2 (2016) 5263. http://dx.doi.org/10.1109/TMBMC.2016.2633265.
[22] N.B. Yanson, A.N. Pavlov, T. Kapitaniak, V.S. Anishchenko, Global reconstruction from nonstationary data, Tech. Phys. Lett. 25 (5) (1999) 412. http://dx.doi.org/10.1134/1.1262500.
[23] Y.I. Molkov, D.N. Mukhin, E.M. Loskutov, R.I. Timushev, A.M. Feigin, Prognosis of qualitative system behavior by noisy, nonstationary, chaotic time series, Phys. Rev. E 84 (2011) 036215. http://dx.doi.org/10.1103/PhysRevE.84.036215.
[24] W. Wang, R. Yang, Y. Lai, V. Kovanis, C. Grebogi, Predicting catastrophes in nonlinear dynamical systems by compressive sensing, Phys. Rev. Lett. 106 (2011) 154101. http://dx.doi.org/10.1103/PhysRevLett.106.154101.

[25] M. Timme, J. Casadiego, Revealing networks from dynamics: An introduction, J. Phys. A 47 (2014) 343001. http://dx.doi.org/10.1088/1751-8113/47/34/343001.
[26] D.A. Smirnov, Quantifying causal couplings via dynamical effects: A unifying perspective, Phys. Rev. E 90 (2014) 062921.
[27] B. Schelter, M. Mader, W. Mader, L. Sommerlade, B. Platt, Y.C. Lai, C. Grebogi, M. Thiel, Overarching framework for data-based modelling, Europhys. Lett. 105 (2014) 30004.
[28] C. Granger, Investigating causal relations by econometric models and cross-spectral methods, Econometrica 37 (3) (1969) 424–438.
[29] L. Baccala, K. Sameshima, Partial directed coherence: A new concept in neural structure determination, Biol. Cybernet. 84 (2001) 463–474.
[30] Y. Chen, G. Rangarajan, J. Feng, M. Ding, Analyzing multiple nonlinear time series with extended Granger causality, Phys. Lett. A 324 (1) (2004) 26–35.
[31] D. Marinazzo, M. Pellicoro, S. Stramaglia, Nonlinear parametric model for Granger causality of time series, Phys. Rev. E 73 (2006) 066216.
[32] M.V. Kornilov, T.M. Medvedeva, B.P. Bezruchko, I.V. Sysoev, Choosing the optimal model parameters for Granger causality in application to time series with main timescale, Chaos Solitons Fractals 82 (2016) 11–21.
[33] R. Hesse, E. Molle, M. Arnold, B. Schack, The use of time-variant EEG Granger causality for inspecting directed interdependencies of neural assemblies, J. Neurosci. Methods 124 (2003) 27–44. http://dx.doi.org/10.1016/S0165-0270(02)00366-7.
[34] M. Sysoeva, E. Sitnikova, I. Sysoev, B. Bezruchko, G. van Luijtelaar, Application of adaptive nonlinear Granger causality: Disclosing network changes before and after absence seizure onset in a genetic rat model, J. Neurosci. Methods 226 (2014) 33–41. http://dx.doi.org/10.1016/j.jneumeth.2014.01.028.
[35] S.G. Shandilya, M. Timme, Inferring network topology from complex dynamics, New J. Phys. 13 (1) (2011) 013004. URL. http://stacks.iop.org/1367-2630/13/i=1/a=013004.
[36] T. Schreiber, Measuring information transfer, Phys. Rev. Lett. 85 (2000) 461.
[37] B. van der Pol, A theory of the amplitude of free and forced triode vibrations, Radio Rev. (later Wireless World) 1 (1920) 701–710.
[38] I.V. Sysoev, V.I. Ponomarenko, D.D. Kulminsky, M.D. Prokhorov, Recovery of couplings and parameters of elements in networks of time-delay systems from time series, Phys. Rev. E 94 (2016) 052207.
[39] W. Liu, K. Ren, S. Meunier-Guttin-Cluzel, G. Gouesbet, Global vector-field reconstruction of nonlinear dynamical systems from a time series with SVD method and validation with Lyapunov exponents, Chin. Phys. 12 (12) (2003) 1366–1373.
[40] A.P. Kuznetsov, E.S. Seliverstova, D.I. Trubetskov, L.V. Turukina, Phenomenon of the van der pol equation, Izvestiya VUZ. Applied Nonlinear Dynamics (Izvestiya Vysshikh Uchebnykh Zavedeniy. Prikladnaya Nelineynaya Dinamika) 22 (4) (2014) 3–42.
[41] W. Addoasah, H. Akpati, R. Mickens, Investigation of a generalized van der pol oscillator differential-equation, J. Sound Vib. 179 (4) (1995) 733–735. http://dx.doi.org/10.1006/jsvi.1995.0048.
[42] I. Kovacic, On the motion of a generalized van der pol oscillator, Commun. Nonlinear Sci. Numer. Simul. 16 (3) (2011) 1640–1649.
[43] R. Stoop, A. Kern, M. Goepfert, D. Smirnov, T. Dikanev, B. Bezruchko, A generalization of the van-der-pol oscillator underlies active signal amplification in drosophila hearing, Eur. Biophys. J. 35 (6) (2006) 511–516. http://dx.doi.org/10.1007/s00249-006-0059-5.
[44] T. Kawahara, Coupled van der pol oscillators — a model of excitatory and inhibitory, Biol. Cybernet. 39 (1980) 37.
[45] D. Linkens, I. Taylor, H. Duthie, Mathematical modeling of the colorectal myoelectrical activity in humans, IEEE Trans. Biomed. Eng. BME-23 (3) (1976) 101.
[46] T. Nomura, S. Sato, S. Doi, J.P. Segundo, M.D. Stiber, A bonhoeffer-van der pol oscillator model of locked and non-locked behaviors of living pacemaker neurons, Biol. Cybernet. 69 (5–6) (1993) 429–437.
[47] J. Lucero, J. Schoentgen, Modeling vocal fold asymmetries with coupled van der pol oscillators, Proc. Meet. Acoust. 19 (2013) 060165.
[48] G. Long, A. Tubis, K. Jones, Modeling synchronization and suppression of spontaneous otoacoustic emissions using van der pol oscillators: Effects of aspirin administration, J. Acoust. Soc. Am. 89 (3) (1991) 1201.
[49] M. Sysoeva, G. Kuznetsova, I. Sysoev, The modeling of rat EEG signals in absence epilepsy in the analysis of brain connectivity, Biophysics (Russian Federation) 61 (4) (2016) 661–669.
[50] A. Pikovsky, Reconstruction of a neural network from a time series of firing rates, Phys. Rev. E 93 (2016) 062313.
[51] Y.I. Molkov, D.N. Mukhin, E.M. Loskutov, A.M. Feigin, G.A. Fidelin, Using the minimum description length principle for global reconstruction of dynamic systems from noisy time series, Phys. Rev. E 80 (2009) 046207. http://dx.doi.org/10.1103/PhysRevE.80.046207.
[52] J. Casadiego, M. Nitzan, S. Hallerberg, M. Timme, Model-free inference of direct network interactions from nonlinear collective dynamics, Nature Commun. 8 (2017) 2192.
[53] J.W. Strutt, The Theory of Sound vol. II, Macmillan, London, 1878, 1896.
[54] R. FitzHugh, Impulses and physiological states in theoretical models of nerve membrane, Biophys. J. 1 (1961) 445–466.
[55] J. Nagumo, S. Arimoto, S. Yoshizawa, An active pulse transmission line simulating nerve axon, Proc. IRE 50 (1962) 2061–2070.
[56] W. Lauterborn, I. Eick, Numerical investigation of a periodically driven laser with an intracavity saturable absorberr, J. Opt. Soc. Amer. B 5 (5) (1988) 1089–1096.
[57] A. Savitzky, M. Golay, Smoothing and differentiation of data by simplified least squares procedures, Anal. Chem. 38 (8) (1964) 1627–1639. http://dx.doi.org/10.1021/ac60214a047.
[58] D.A. Smirnov, B.P. Besruchko, Spurious causalities due to low temporal resolution: Towards detection of bidirectional coupling from time series, Europhys. Lett. 100 (2012) 10005.
[59] N. Wiener, The theory of prediction, in: E.F. Beckmann (Ed.), Modern Mathematics for the Engineer, McGraw-Hill, New York, 1956.
[60] W.X. Wang, R. Yang, Y.C. Lai, V. Kovanis, M. Harrison, Time-seriesbased prediction of complex oscillator networks via compressive sensing, Europhys. Lett. 94 (2011) 48006. http://dx.doi.org/10.1209/0295-5075/94/48006.
[61] A. Lüttjohann, G. van Luijtelaar, The dynamics of cortico-thalamo-cortical interactions at the transition from pre-ictal to ictal LFPs in absence epilepsy, Neurobiol Dis 47 (2012) 47–60. http://dx.doi.org/10.1016/j.nbd.2012.03.023.
[62] F. Gerhard, G. Pipa, B. Lima, S. Neuenschwander, W. Gerstner, Extraction of network topology from multi-electrode recordings: Is there a small-world effect? Front. Comput. Neurosci. 5 (2011) 4. http://dx.doi.org/10.3389/fncom.2011.00004.
[63] A. Porta, L. Faes, Wiener–Granger causality in network physiology with applications to cardiovascular control and neuroscience, Proc. IEEE (2015). http://dx.doi.org/10.1109/JPROC.2015.2476824.
[64] M. Sysoeva, A. Lüttjohann, G. van Luijtelaar, I. Sysoev, Dynamics of directional coupling underlying spike-wave discharges, Neuroscience 314 (2016) 75–89. http://dx.doi.org/10.1016/j.neuroscience.2015.11.044.
[65] M. Sysoeva, L. Vinogradova, G. Kuznetsova, I. Sysoev, C. van Rijn, Changes in corticocortical and corticohippocampal network during absence seizures in WAG/Rij rats revealed with time varying Granger causality, Epilepsy Behav. 64 (2016) 44–50. http://dx.doi.org/10.1016/j.yebeh.2016.08.009.
[66] M. Sysoeva, E. Sitnikova, I. Sysoev, Thalamo-cortical mechanisms of initiation, maintenance and termination of spike-wave discharges at WAG/RIJ rats, Zh Vyssh Nerv Deiat Im I P Pavlova 66 (1) (2016) 103–112.
[67] I.I. Mokhov, D.A. Smirnov, El niño — southern oscillation drives north atlantic oscillation as revealed with nonlinear techniques from climatic indices, Geophys. Res. Lett. 33 (2006) L03708. http://dx.doi.org/10.1029/2005GL024557.
[68] A. Builes-Jaramillo, N. Marwan, G. Poveda, J. Kurths, Nonlinear interactions between the amazon river basin and the tropical north atlantic at interannual timescales, Clim. Dynam. 50 (7–8) (2018) 29512969.
[69] C. Hiemstra, J.D. Jones, Testing for linear and nonlinear Granger causality in the stock price-volume relation, J. Finance 49 (5) (1994) 1639–1664. http://dx.doi.org/10.1111/j.1540-6261.1994.tb04776.x.